Int. J. Electrochem. Sci., 10 **(2015)** 9286 - 9296

International Journal of
ELECTROCHEMICAL
SCIENCE
www.electrochemsci.org

Anodic TiO_2 Nanorod Arrays and Surface Wettability

Sorachon Yoriya[*] *and Angkana Chumphu*

National Metal and Materials Technology Center, 114 Thailand Science Park, Phahonyothin Road, Khlong 1, Khlong Luang, PathumThani 12120, Thailand
[*]E-mail: sorachy@mtec.or.th

Received: 26 August 2015 / *Accepted:* 7 September 2015 / *Published:* 30 September 2015

We report a discovery of titanium dioxide nanorods that could be directly fabricated by electrochemical anodization in diethylene glycol medium. The anodization has been strictly performed in a particular condition using electrolyte mixture containing hydrofluoric acid and water, low anodization voltage, and controlled temperature bath at 20°C, consequently yielding TiO_2 nanorod arrays with size range of 30-50 nm. Analysing the current density slope, our finding has shown that the possible window to produce titania nanorod structure is limited by the rate of increment in current density, which is less than 10 $\mu A/cm^2/h$. The DEG-fabricated TiO_2 nanorod array has exhibited the hydrophobic characteristic surface property with contact angles higher than 70°, different than those commonly observed for the TiO_2 nanotube array films grown in other organic electrolytes. Surface wettability relating to the array morphologies has been investigated. A schematic drawing demonstrated different views of relation among surface wettability, architectural morphologies, and electrolyte property.

Keywords: TiO_2 nanorod arrays, low voltage, diethylene glycol, surface wettability

1. INTRODUCTION

Highly ordered vertically oriented TiO_2 nanotube arrays, fabricated by electrochemical anodization of titanium in fluoride-based electrolytes, have shown their great ability in dye-sensitized solar cells,[1, 2] water-photoelectrolysis,[3-5] and high-performance sensors.[6-8] The efficiency of devices is primarily determined by the nanotube architectures and properties, which are known to be achieved by strictly manipulating electrolyte composition and anodization parameters. Employing nanotubular structure with particularly controlled surface properties, the titania nanotube arrays have attracted considerable attention during the past years for use in biomedical applications due to their bioactivity and biocompatibility properties. The nanotubular geometry of TiO_2 with specific

dimensions can be exploited in tissue engineering,[9, 10] drug eluting coatings for medical implants,[11-13] growth platform for stem cell,[14, 15] and bone cell,[16-19] and blood clotting.[20-22] For bone-material interface, the bone growth level is dependent upon the surface characteristics of the implant. Proper surface chemistry and topography are believed to play a critical role influencing the extent of osseointegration, governing long-term stability and functionality of the implant.[16, 18] While in the application of bone regeneration, superhydrophilicity of TiO_2 nanotube array is needed because the nanotube feature and surface wettability has been believed to promote the greater cell adhesion.[19] Blood compatibility of TiO_2 nanotube arrays makes them beneficial for blood compatible coating on surgical tools, due to their inactive surface and chemical stability that help to retain the natural forms of proteins and also reduce unwanted the number of platelet activation. [16] Wettability of material surface is an important factor that is anticipated to possess good blood compatibility in terms of controllable clotting kinetics and clotting strength, adhesion and activation of platelets.[23] In blood vessel replacement and wound management, superhydrophobic surface is strongly preferred to prevent platelets adhesion, as altering surface chemical composition can be practically performed for titanium implants to improve the surface characteristic.[24] To alter the surface characteristic of TiO_2 nanotube array film, generally surface activation has been employed to achieve the excellent bioactivity. Surface treatment by applying chemicals of different polarity on the film surface is known a controllable way to achieve the superhydrophobic material, while the superhydrophilic surface could be obtained by exposing the titania nanotube film with UV light.[22] To our best knowledge, it is difficult to obtain superhydrophobic and superhydrophilic characteristics of TiO_2 nanotube array surface without any further surface modification. In addition, it has been believed that the material surface for implantation has random topography as those fabricated nanofeatures could be reproducible controlled.[18] To this particular point, clarification is needed for a better insight into the effect of surface topography on wettability of the film.

In this work, we report on a window of electrochemical anodization process that could provide possibility to produce the TiO_2 nanoarray films− nanotube and nanorod arrays, with different features and surface wettability using the same anodizing electrolyte. This work shows how to manipulate anodizing parameters to step over the capability window of producing nanotubular structure of anodic oxide film. It is of great significance to the point describing a limiting synthesis window for the nanorod array critically controlled the oxide formation; the TiO_2 nanorod array has been achieved. Observation of anodization current in DEG is also discussed, with its current behavior, current density flux corresponding anodization rate to be analyzed. Further, we investigate water contact angle of the TiO_2 nanorod array films in comparison to that of the TiO_2 nanotube array films. Preferred nanoarray architecture of the titania film relating to its surface wettability is explained.

2. EXPERIMENTAL

Titanium foil (250 μm thick, 99.7%; Sigma-Aldrich) was cut in a size of 1.0 cm × 2.0 cm, then cleaned with acetone, soap and iso-propanol. Anodizing electrolytes were prepared using different organic electrolyte media; (i) glycerol (99%, Aldrich)-x_1 % ammonium fluoride (98%, Merck)-30%

H_2O; x_1 %=1-2%, (ii) diethylene glycol (DEG, 99.7%, Sigma-Aldrich)-hydrofluoric (HF, 48% solution, Merck)-3% water, and (iii) ethylene glycol (EG, 99.%; Sigma Aldrich))-x_2% ammonium fluoride (98%, Merck)-3% H_2O; x_2=0.15-1%. Anodization was performed upon varying parameters in a controlled temperature water bath at 20°C using a two-electrode electrochemical cell and platinum foil as cathode electrode. Morphology of the anodized films was characterized by scanning electron microscope (SEM, JEOL JSM–6301F). Water drop contact angle was measured by optical contact angle meter (DataPhysics, OCA-40) at ambient temperature, with volume size of water droplet fixed at 1 μl.

3. RESULT AND DISCUSSION

Considering the effect of high field model, the film growth rate is limited by migration of ionic species, e.g. Ti^{4+} and O^{2-}, through the oxide film.[25] [26-29] The physical properties of electrolyte in terms of viscosity, conductivity, as well as intermolecular hydrogen bonding could act their dominant role affecting the ionic mobility towards the electrode,[30] consequently determining the anodic current and the growth of nanotube. The anodic current is expressed as $I=nFJ$, where I, n, F, and J are, anodic current, number of electrons transporting in the reaction, Faraday constant, and flux of ions. In relation to porous structure formation, the anodization current-time response during anodization was monitored. Figure 1 (a) shows the current-time behavior of titanium foil samples anodized in DEG electrolyte containing 2%HF and 3 % H_2O at different applied voltages. The anodization current behavior seen in Figure 1 (a) are typical for the titanium anodization in DEG, observed different than those seen in other organic electrolytes as a function of voltage and fluoride species.[4, 25, 31-35] The linear increase in current density was observed for all voltages during the first 16 h period of anodization, as a linear diffusion of ionic species is also assumed to occur in this electrolyte along a concentration gradient from bulk to the oxide layer surface. After the 16 h, fluctuation of current density is clearly seen, probably due to the developed conductivity of electrolyte as a function of time becoming the predominant governing the anodization reactions.[36] At higher voltage, the drastic drop of current density is seen more clearly.

Under potentiostatic anodization, the field strength decreases with the film thickness, leading to the ionic current dropping with time and the smaller growth rate. The current decrease is controlled by diffusion of ionic species, electrolyte composition and its conductivity.[29, 37, 38] In addition, the current density varies depending upon the surface of metal substrate.[39] If surface is rough, the smoothing process occurs by reducing the surface area of the metal substrate. Variation of current density requires necessary changes in the atomic migrations of metal and oxygen atoms and the formation of oxide structure accordingly.

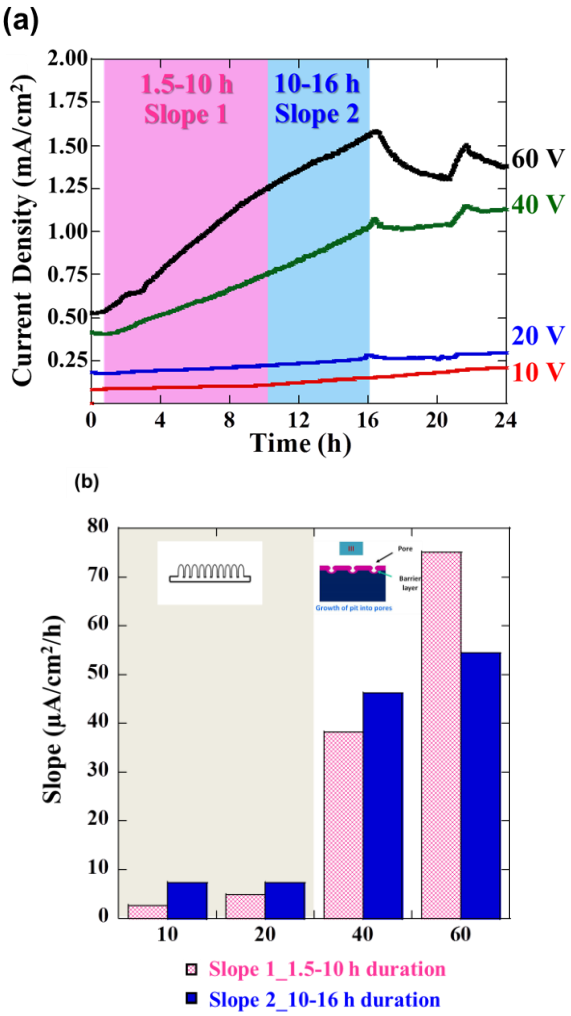

Figure 1. (a) Plots of current density vs. anodization time of titanium foil samples anodized in DEG-2%HF-3%H_2O electrolyte for 24 h at different voltages. (b) Plots of slopes of each voltage determined from those curves in Figure 1 (a) during the anodization periods of 1.5-10 h (Slope 1) and 10-16 h (Slope 2).

For a given electrolyte composition, the rate of reaction in terms of flux is potential dependent,

$$\frac{i}{nFA} = k_f C_0(x = 0)$$

where k_f is potential-dependent rate constant, $C_O(x=0)$ is concentration of oxidized species at the interface, and A is surface area.[29] In this study, slope of the current density-time plots was examined over the 16 h duration, with two stages of slope determined over the periods of 1.5-10 h (Slope 1) and 10-16 h (Slope 2). The proportionality constants were plotted against the applied voltage and shown in Figure 1 (b). The determined slopes are less than 10 μA/cm^2/h for the 10 V and 20 V conditions, and at least 40 μA/cm^2/h for the 40 V and 60 V conditions. The values indicate the rate of mass transport expressing in relation of flux to the ionic concentration driving force due to diffusion and migration.[40] Anodizing in the DEG at low voltage, the reaction is mainly dominated by the field assisted oxidation and dissolution; the slow diffusion determining the transport-controlled reactions could govern the dissolution rate. Using higher voltage, a combination role of improved conductivity

facilitating the dissolution rate becomes more significant at prolonged period, thus reflecting the behavior that Slope 2 is comparatively lower than Slope 1. This is attributed to the rate of mass transfer for oxide formation resisted by the dissolution effect playing a major contribution to the total growth rate of the oxide film. The decrease in slope is believed to be due to the key factor of dissolution rate promoting pore organization.[29, 41]

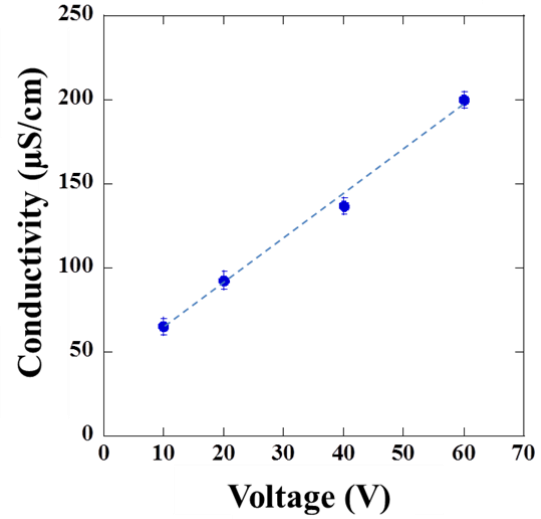

Figure 2. A plot of electrolyte conductivity measured after anodization and voltage for Ti anodization in DEG–2% HF-3% H_2O electrolytes for 24 h.

Conductivity of the anodized electrolytes was examined as a function of voltage, plotted in Figure 2. For titanium anodization in DEG–2% HF-3% H_2O, the linear increase in electrolyte conductivity directly proportional to the applied anodization potential is similar to that reported for the titanium anodization in other DEG composition.[36, 42] The increased conductivity with voltage is attributed to the field assisted dissolution governing the process, leading to the more Ti^{4+} migration at the metal/oxide interface. Due to more free ions dissolving in the electrolyte, those ionic species could in turn facilitate more transport charges to the oxide layer, consequently promoting titanium dissolution from the oxide wall into the electrolyte.[31, 36] The electrolyte conductivity κ can be explained in terms of its proportion to Z_i−charge number of ion i, u_i−electric mobility of ion i, and concentrations c of the constituent ions (ion i) for dilute electrolyte solutions: $\kappa=\sum | Z_i | F u_i c_i$.[43] [43] In Figure 2, the conductivity values measured for all voltage conditions are in the range of 200 µS/cm. The conductivity per voltage ratio to be proposed for the DEG–2% HF-3% H_2O electrolyte is nominally 2.64 µS cm^{-1} V^{-1}, higher than 1.08 µS cm^{-1} V^{-1} [36] for the DEG–2% HF without water addition. Incorporation of polar additives into DEG has confirmed its role enhancing total conductivity of the anodizing electrolyte. It is critical for the reaction atmosphere of viscous electrolyte system like DEG that the transport of reactants to the electrode surface could be limited by the concentration gradients, as the concentration gradient along the channels is considerably significant in the growth of nanopores. Among the organic electrolytes normally used for anodization, the average growth rate in DEG electrolyte was found as 0.1-0.3 µm h^{-1}, considered slowest compared to those reported for DMSO (1 µm h^{-1}), FA (2 µm h^{-1}), and EG (15 µm h^{-1}) electrolytes.[4, 25, 37, 44]

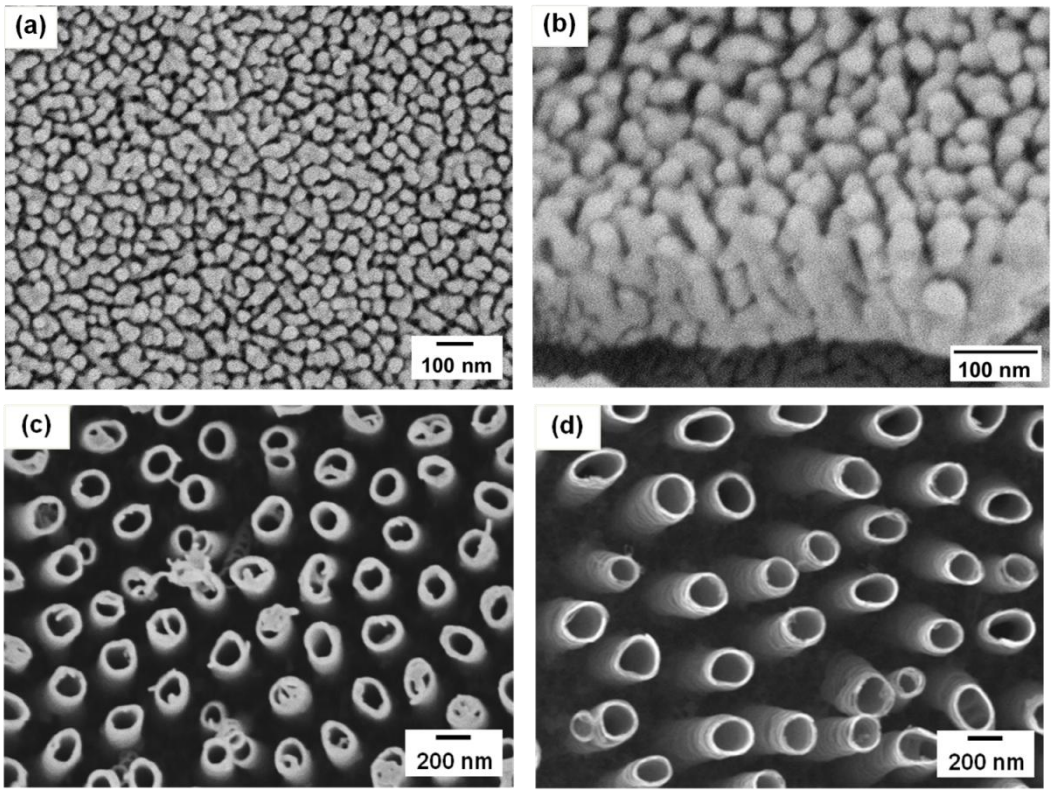

Figure 3. FESEM images of TiO_2 films anodized in DEG–2% HF-3% H_2O electrolyte for 24 h, showing (a) top view and (b) cross-sectional views of TiO_2 nanorod array as using 20 V, and TiO_2 nanotube array as using (c) 40 V and (d) 60 V.

Microscopic study has revealed an interesting achievement, reported for the first time that the DEG–2% HF-3% H_2O electrolyte is capable of growing the TiO_2 nanorod array film *via* a facile anodization process. Using low voltage, the particular conditions of 10 V and 20 V demonstrated their potential for the formation of TiO_2 nanorod array with max. thickness ~ 300 nm; see Figure 3 (a)-(b). Those irregular-shaped nanorods are vertically aligned and freely standing on the oxide barrier layer over the titanium substrate. Confirming this achievement in the slow rate condition, the formation of the nanorod structure is limited to the transfer-determining rate of 10 $\mu A/cm^2/h$, 4 times lower than the rate of pore pitting to form the typical tubular structure, according to those illustrated in Figure 1 (b). Further increase in voltage, the TiO_2 nanotube array films with commonly obtained morphology were observed; see Figure 3 (c)-(d). The pore diameter of TiO_2 nanotubes grown at 40 V and 60 V is in the approximate range of 200 nm, and the nanotube length of those anodized samples is 2 μm. The anodization voltage is believed to play a significant role in controlling the pore diameter; discrepancy of the pore cell could be explained by dissolution efficiency at the oxide wall as depending upon electrolyte properties. Dissolution at the top part to prevent nanotube pore clogging is strongly influenced by the addition of water to the organic electrolyte.[45]

To investigate surface property of those nanoarray films, water drop contact angle measurement was carried out. Figure 4 (a) shows the water drop contact angles of the TiO_2 nanoarray films grown in DEG electrolyte plotted as a function of voltage. Under the same window of electrolyte medium and

voltage, a large difference in contact angle was observed from two surface characteristics of the films; ~20° for the nanotube array films and ~100° for the nanorod array film, exhibiting hydrophilic and hydrophobic characteristics, respectively. It is evident that either intrinsically hydrophilic or hydrophobic surface behavior could be obtained directly from DEG anodization bath, without further chemical post-treatment. For the titania nanotube array films grown in glycerol and ethylene glycol mixtures, the contact angles were found to fall in the hydrophilic range of 10°-30°; see Figure 4 (b) and (c). Using glycerol-based electrolyte, the contact angle tends to slightly decrease with voltage. We speculate that electrolyte modification as well as proper manipulation of anodizing parameters may enhance possibility to reach the superhydrophilic level. While for the EG-based electrolyte, the contact angles found for the achieved TiO_2 nanoarray films remain unchanged over the variation range of voltage from 20-60 V. In EG, the anodization voltage did not show its role to differ the contact angle. The architectural topology of nanofeatures grown in the low-ranged conductivity is believed an important factor determining the surface wettability of the anodized film.

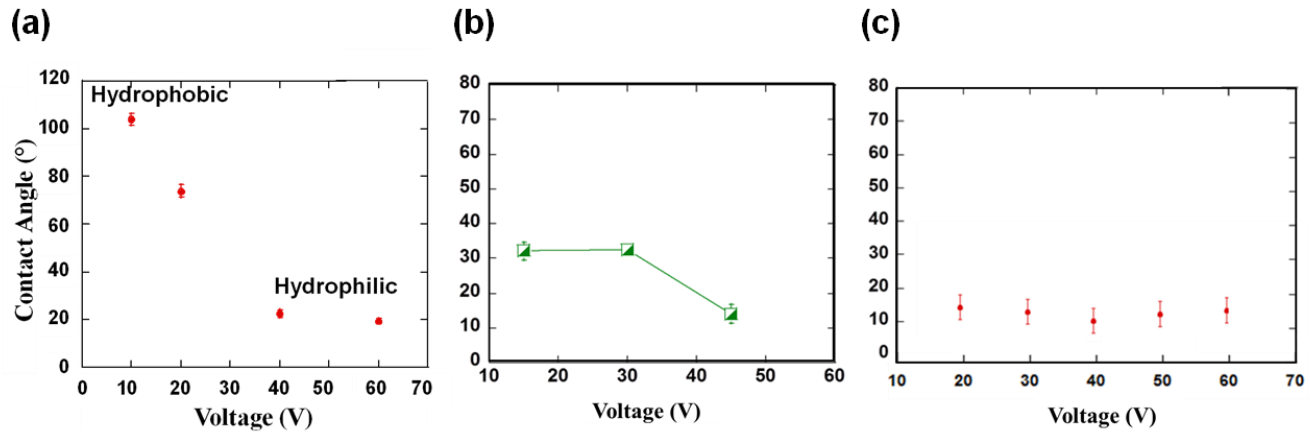

Figure 4. Water drop contact angle values of TiO_2 nanoarray films grown in (a) DEG–2% HF-3% H_2O electrolytes for 24 h, (b) glycerol-1.5 wt.%NH_4F-30% H_2O electrolytes for 1 h, and (c) EG-0.3% NH_4F-3% H_2O electrolytes for 24 h. Those nanoarray films were annealed at 530 ºC for 3 h. Pore size of the nanotube samples used in this measurement is in the range of 200-300 nm. Conductivity range measured for Figure (a)-(c) is approximately 200, 500, and 1600-2500 μS/cm, respectively.

Figure 5 shows a schematic diagram demonstrating surface wettability and corresponding morphological features of the anodized TiO_2 nanoarray films obtained in DEG, EG, and glycerol. The growth characteristic nature of EG electrolyte is the pattern defined as ideally hexagonal close-packing, while the orientation observed for both glycerol and DEG is known the discrete, well-separated nanotubes.[42] The role of electrolyte medium and their kinetics in determining the nanotube morphology and properties are considerably important. Observed from the mapping, both hydrophobic and hydrophilic surface of the anodized films could be obtained in the conductivity range of 2500 μS/cm. The ordering degree seems to have unspecified relation to conductivity of the anodizing electrolyte. The highly ordered, ideally closed packing array of nanotubes could be obtained mostly in the EG electrolyte with the particular conductivity around 500 μS/cm, and DEG containing large

cation size of fluoride bearing species.[42] Approach to obtaining the nanofeatures with either superhydrophobicity or superhydrophilicity could be possible by manipulating electrolyte conductivity with a proper selection of electrolyte medium and composition.

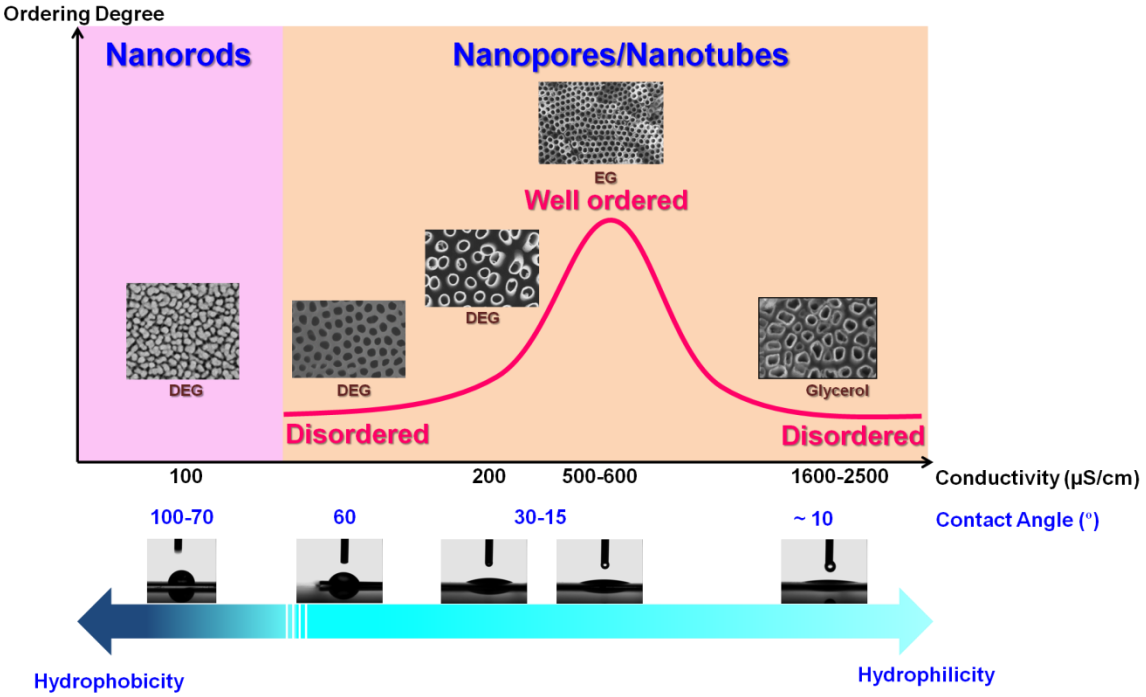

Figure 5. Surface wettability regime proposed for the anodized TiO_2 nanoarray films of different architecture obtained in different organic electrolyte mediums.

The fast growth rate condition, either due to the large concentration of ionic movement or the use of high voltage, is presumably an important factor involving the change in oxide composition of titania nanotube arrays. The large fraction of anion species composition could probably yield the surface that is prone to be hydrophilic. In the titanium dioxide film, the ionic current is carried by the titanium cation and oxygen anion, with 60 % of current density involving the formation of TiO_2,[46] where only O^{2-} involving the oxide formation process.[47] Whereas 40 % current efficiency was assumed to correspond to TiO_2 dissolution. At the oxide/electrolyte interface, the acid electrolyte will try to remove the kink site of anions and cations from the oxide surface.[48] In area closed to the oxide/electrolyte interface, the O^{2-} concentration is high and the Ti^{4+} concentration is low.[49] Normally the large anion O^{2-} cannot move inward to the pore bottom, but a high field can pull the O^{2-} ion back through the oxide layer into the interstitial position. Also the field is sufficiently high to prevent movement of cations against the field direction.[50] Thus, the oxide composition change may occur from the addition of O^{2-} into the oxide, where OH^- is acidified at the oxide/electrolyte interface: $OH^-_{aq} \rightleftharpoons O^{2-}_{OX} + H^+_{aq}$. Hoar and Mott suggested that OH^- ion is produced by the field-assisted process during the formation of porous oxide film.[48] Patermarakis and Moussoutzanis suggested that the OH^- anion is more likely to migrate along intercrystalline surface like O^{2-}, rather than through vacancies inside the crystallites.[51] The OH^- migrates slower than O^{2-} due to the lower charge

movement; hence, the rate of oxide formation for OH^- is insignificant with respect to that of O^{2-}. While H^+ migration may take place as well during the oxide growth depending upon the electrolyte concentration. In terms of high current density, the growth efficiency tends to decrease caused by (i) the substantial effects of film dissolution, (ii) the accessible fluoride ion from the electrolyte, and (iii) the increased amount of proton within the pores due to the increased acidity of electrolyte. When the rate of oxide formation decreases, the thickness of barrier layer also decreases. Due to the reversible absorption and desorption of proton in the film, the structure of the oxide film was found to contain a large number of hydroxyl bridges at which the composition is represented by TiO_2 $(H_2O)_{1.4}$ or $TiO_{0.6}(OH)_{2.8}$.[52, 53]

4. CONCLUSION

This work presented the fabrication of TiO_2 nanoarray features in selected organic electrolytes, providing crucial information on how electrolyte properties and anodization parameters strongly affect the growth architecture and the surface wettability of the oxide nanoarray. The result showed that either hydrophilic or hydrophobic surface could be obtained directly by a facile anodization process, without any surface treatment. The TiO_2 nanorod array exhibiting hydrophobic could be achieved in the low voltage and low conductivity conditions. While the commonly obtained TiO_2 nanotube array films were found to be hydrophilic. Anodization at higher voltage facilitating the rate of reactions is believed to govern the oxide composition and thus provide the titania nanotube array with intrinsically hydrophilicity. The current density behavior in DEG electrolyte was investigated and evaluated as a function of voltage. The mass transfer-determining rate for growing the TiO_2 nanorod array film was found limited to 10 $\mu A/cm^2/h$. The conductivity of the anodized electrolyte was found to increase in a linear relation to the applied voltage. The proposed schematic drawing revealed that surface characteristic is mainly dependent upon architecture of the oxide film, which is a consequent effect of varying ionic content, conductivity, and anodization voltage. It was assumed for the fast growth rate that could play a critical role controlling the oxide formation, leading to various composition along the tube wall surface, eventually determining surface characteristic property of the anodized TiO_2 film. For potential use in biomedical applications, one may suggest as an alternative pathway of material selection that, building upon this work, development of architectures of TiO_2 nanoarray platform to possess excellent bioactivity such as hemocompatibility could be possible.

ACKNOWLEDGEMENTS
The authors acknowledge the National Metal and Materials Technology Center (MTEC), Thailand, for instrument facilities and providing research funding Grant no. P1100228 through the Ceramics Technology Research Unit.

References

1. G. K. Mor, K. Shankar, M. Paulose, O. K. Varghese and C. A. Grimes, *Appl. Phys. Lett.* 91 (2007) 152111.

2. D. Kuang, J. r. m. Brillet, P. Chen, M. Takata, S. Uchida, H. Miura, K. Sumioka, S. M. Zakeeruddin and M. Gratzel, *ACS Nano,* 2 (2008) 1113.
3. M. Paulose, G. K. Mor, O. K. Varghese, K. Shankar and C. A. Grimes, *J. Photochem. Photobio. Chem.* 178 (2006) 8.
4. K. Shankar, G. K. Mor, H. E. Prakasam, S. Yoriya, M. Paulose, O. K. Varghese and C. A. Grimes, *Nanotechnol.* 18 (2007) 065707; 11 pages.
5. R. P. Lynch, A. Ghicov and P. Schmuki, *J. Electrochem. Soc.* 157 (2010) G76.
6. Y. Y. Song and P. Schmuki, *Electrochem. Comm.* 12 (2010) 579.
7. S. Park, S. Kim, S. Park, W. I. Lee and C. Lee, *Sensors,* 14 (2014) 15849.
8. S. Lin and D. Li, *Sens. Actuator B: Chem.* 156 (2011) 505.
9. K. C. Popat, E. E. L. Swan, V. Mukhatyar, K. I. Chatvanichkul, G. K. Mor, C. A. Grimes and T. A. Desai, *Biomater.* 26 (2005) 4516.
10. T. Dey, P. Roy, B. Fabry and P. Schmuki, *Acta Biomater.* 7 (2011) 1873.
11. K. C. Popat, M. Eltgroth, T. J. La Tempa, C. A. Grimes and T. A. Desai, *Small* 3 (2007) 1878.
12. L. L. Peng, A. D. Mendelsohn, T. J. LaTempa, S. Yoriya, C. A. Grimes and T. A. Desai, *Nano Letters* 9 (2009) 1932.
13. Y. Hu, K. Cai, Z. Lue, D. Xu, D. Xie, Y. Huang, W. Yang and P. Lie, *Acta Biomater.* 8 (2012) 439.
14. J. Park, S. Bauer, K. von der Mark and P. Schmuki, *Nano Lett.* 7 (2007) 1686.
15. L. Lv, Y. Liu, P. Zhang, X. Zhang, J. Lie, T. Chen, P. Su, H. Li and Y. Zhou, *Biomater.* 39 (2015) 193.
16. K. C. Popat, L. Leoni, C. A. Grimes and T. A. Desai, *Biomater.* 28 (2007) 3188.
17. K. C. Popat, K. I. Chatvanichkul, G. L. Barnes, T. J. Latempa, C. A. Grimes and T. A. Desai, *J. Biomed. Mat. Res. Part A 80A* (2007) 955.
18. W.-q. Yu, X.-q. Jiang, F.-q. Zhang and L. Xu, *J. Biomed. Mat. Res. A* 94 (2010) 1012.
19. K. S. Brammer, C. J. Frandsen and S. Jin, *Trends Biotech.* 30 (2012) 315.
20. S. C. Roy, M. Paulose and C. A. Grimes, *Biomater.* 28 (2007) 4667.
21. S. C. Roy, K. G. Ong, K. Zeng and C. A. Grimes, *Sensor Lett.* 5 (2007) 432.
22. Y. Yang, Y. Lai, Q. Zhang, K. Wu, L. Zhang, C. Lin and P. Tang, *Colloids Surf. B: Biointerfaces* 79 (2010) 309.
23. B. S. Smith, S. Yoriya, L. Grissom, C. A. Grimes and K. C. Popat, *J. Biomed. Mat. Res. Part A* 95A (2010) 350.
24. M. Ma and R. M. Hill, *Curr. Opin. Colloid Interface Sci.*11 (2006) 193.
25. H. E. Prakasam, K. Shankar, M. Paulose, O. K. Varghese and C. A. Grimes, *J. Phys. Chem. C* 111 (2007) 7235.
26. D. Gong, C. A. Grimes, O. K. Varghese, W. C. Hu, R. S. Singh, Z. Chen and E. C. Dickey, *J. Mat. Res.* 16 (2001) 3331.
27. C. A. Grimes and G. K. Mor, TiO_2 Nanotube Arrays: *Synthesis, Properties, and Applications* Springer, New York (2009).
28. W. Lee, R. Ji, U. Gosele and K. Nielsch, *Nature Mat.* 5 (2006) 741.
29. K. Yasuda and P. Schmuki, *Electrochim. Acta* 52 (2007) 4053.
30. C. M. Kinart, A. C´wiklin´ska, M. Maja and W. J. Kinart, *Fluid Phase Equilibria* 262 (2007) 244.
31. K. Shankar, G. K. Mor, A. Fitzgerald and C. A. Grimes, *J. Phys. Chem. C* 111 (2007) 21.
32. S. Berger, J. Kunze, P. Schmuki, A. T. Valota, D. J. LeClere, P. Skeldon and G. E. Thompson, *J. Electrochem. Soc.* 157 (2010) C18.
33. S. Li, G. Zhang, D. Guo, L. Yu and W. Zhang, *J. Phys. Chem. C* 113 (2009) 12759.
34. D. Regonini, C. R. Bowen, R. Stevens, D. Allsopp and A. Jaroenworaluck, *Phys. Stat. Sol. a* 204 (2007) 1814.
35. C. M. Ruan, M. Paulose, O. K. Varghese, G. K. Mor and C. A. Grimes, *J. Phys. Chem. B* 109 (2005) 15754.

36. S. Yoriya and C. A. Grimes, *J. Mat. Chem.* 21 (2011) 102.
37. S. Yoriya, M. Paulose, O. K. Varghese, G. K. Mor and C. A. Grimes, *J. Phys. Chem. C* 111 (2007) 13770.
38. A. Valota, D. J. LeClerea, P. Skeldona, M. Curionia, T. Hashimotoa, S. Berger, J. Kunzeb, P. Schmuki and G. E. Thompsona, *Electrochim. Acta* 54 (2009) 4321.
39. J. P. S. Pringle, *Electrochim. Acta* 25 (1980) 1403.
40. G. Prentice, *Electrochemical Engineering Principles* Prentice Hall, New Jersey (1991).
41. S. Yoriya and N. Bao, *Int.. J. Electrochem. Sci.* 9 (2014) 7182.
42. S. Yoriya, G. K. Mor, S. Sharma and C. A. Grimes, *J. Mat. Chem.* 18 (2008) 3332.
43. K. Izutsu, *Electrochemistry in Nonaqueous Solutions* Wiley-VCH, New York (2002).
44. M. Paulose, K. Shankar, S. Yoriya, H. E. Prakasam, O. K. Varghese, G. K. Mor, T. A. Latempa, A. Fitzgerald and C. A. Grimes, *J. Phys. Chem. B* 110 (2006) 16179.
45. J. M. Macak, H. Hildebrand, U. Marten-Jahns and P. Schmuki, *J. Electroanal. Chem.* 621 (2008) 254.
46. D. J. LeClere, A. Velota, P. Skeldon, G. E. Thompson, S. Berger, J. Kunze, P. Schmuki, H. Habazaki and S. Nagata, *J. Electrochem. Soc.*155 (2008) C487.
47. F. Thebault, B. Vuillemin, R. Oltra, J. Kunze, A. Seyeux and P. Schmuki, *Electrochem. Sol. Stat. Lett.* 12 (2009) C5.
48. T. P. Hoar and N. F. Mott, *J. Phys. Chem. Sol.* 9 (1959) 97.
49. L. V. Taveira, J. M. Macak, H. Tsuchiya, L. F. P. Dick and P. Schmuki, *J. Electrochem. Soc.* 152 (2005) B405.
50. J. W. Diggle, T. C. Downie and C. W. Goulding, *Chem. Rev.* 69 (1969) 365.
51. G. Patermarakis and K. Moussoutzanis, *Electrochim. Acta* 40 (1995) 699.
52. T. Ohtsuka, M. Masuda and N. Sato, *J. Electrochem. Soc.* 132 (1985) 787.
53. C. K. Dyer and S. S. L. Leach, *Electrochim. Acta* 23 (1978) 1387.